



# Infection by the parasitic helminth *Trichinella spiralis* activates a Tas2r-mediated signaling pathway in intestinal tuft cells

Xiao-Cui Luo<sup>a</sup>, Zhen-Huang Chen<sup>a</sup>, Jian-Bo Xue<sup>a</sup>, Dong-Xiao Zhao<sup>a</sup>, Chen Lu<sup>a</sup>, Yi-Hong Li<sup>a</sup>, Song-Min Li<sup>a</sup>, Ya-Wen Du<sup>a</sup>, Qun Liu<sup>a</sup>, Ping Wang<sup>b</sup>, Mingyuan Liu<sup>c,d</sup>, and Liqun Huang<sup>a,e,1</sup>

<sup>a</sup>College of Life Sciences, Zhejiang University, 310058 Hangzhou, China; <sup>b</sup>Biosensor National Special Lab, Key Lab for Biomedical Engineering of Ministry of Education, Department of Biomedical Engineering, Zhejiang University, 310027 Hangzhou, China; <sup>c</sup>Key Lab of Zoonosis Research, Institute of Zoonosis, Jilin University, 130062 Changchun, China; <sup>d</sup>College of Veterinary Medicine, Jilin University, 130062 Changchun, China; and <sup>e</sup>Monell Chemical Senses Center, Philadelphia, PA 19104

Edited by Lora V. Hooper, The University of Texas Southwestern, Dallas, TX, and approved February 4, 2019 (received for review July 27, 2018)

The parasitic helminth *Trichinella spiralis*, which poses a serious health risk to animals and humans, can be found worldwide. Recent findings indicate that a rare type of gut epithelial cell, tuft cells, can detect the helminth, triggering type 2 immune responses. However, the underlying molecular mechanisms remain to be fully understood. Here we show that both excretory–secretory products (E–S) and extract of *T. spiralis* can stimulate the release of the cytokine interleukin 25 (IL-25) from the mouse small intestinal villi and evoke calcium responses from tuft cells in the intestinal organoids, which can be blocked by a bitter-taste receptor inhibitor, allyl isothiocyanate. Heterologously expressed mouse Tas2r bitter-taste receptors, the expression of which is augmented during tuft-cell hyperplasia, can respond to the E–S and extract as well as to the bitter compound salicin whereas salicin in turn can induce IL-25 release from tuft cells. Furthermore, abolishment of the G-protein  $\gamma 13$  subunit, application of the inhibitors for G-protein  $\alpha/i$ , G $\beta$  subunits, and phospholipase C $\beta 2$  dramatically reduces the IL-25 release. Finally, tuft cells are found to utilize the inositol triphosphate receptor type 2 (I $p_{3r2}$ ) to regulate cytosolic calcium and thus Trpm5 activity, while potentiation of Trpm5 by a sweet-tasting compound, stevioside, enhances tuft cell IL-25 release and hyperplasia in vivo. Taken together, *T. spiralis* infection activates a signaling pathway in intestinal tuft cells similar to that of taste-bud cells, but with some key differences, to initiate type 2 immunity.

$\alpha$ -gustducin | G $\alpha$  | G $\beta 1\gamma 13$  | I $p_{3r2}$  | type 2 immunity

The mammalian gut epithelium is a single layer of cells that covers the luminal surface of the intestine. The function of the epithelial cells includes not only absorbing nutrients and forming a barrier to protect the rest of the body but also communicating with the gut microbiota that comprises an enormous number of commensal, symbiotic, and pathogenic microorganisms such as viruses, archaea, bacteria, fungi, and parasitic helminths (1, 2). A growing body of evidence has shown that the crosstalk between the gut epithelial cells and microbiome has profound impact on the host's physiology and health (3–6).

Recent studies indicate that a rare type of intestinal epithelial cells, tuft cells, provides a critical link to the infection of viruses, protozoa, and helminths (7–11) as well as to the alterations in the gut microflora (12). Upon activation by some unknown signals from parasitic nematodes such as *Nippostrongylus brasiliensis* and *Heligmosomoides polygyrus* or the protozoan *Trichuris muris*, sparse tuft cells initiate an intracellular signaling cascade, leading to the release of interleukin 25 (IL-25), which directly acts on intestinal type 2 innate lymphoid cells (ILC2s) in the lamina propria to secrete interleukin 13 (IL-13). In turn, IL-13 directs stem and progenitor cells in the crypt to proliferate and preferentially differentiate into tuft and goblet cells, leading to the “weep and sweep” response including mucus secretion and parasite expulsion from the gut.

Thus, this feed-forward circuit of the immune response consists of tuft cells, IL-25 release, ILC2s, IL-13 production, tuft-

and goblet-cell hyperplasia, and final elimination of the parasites (8–13). How the initial few sentinel tuft cells detect and respond to the parasite invasion appears to be the key to the steps to switch on the circuit. Gene expression analyses found that tuft cells express some taste-signaling proteins, suggesting that tuft cells are chemosensory cells that may employ taste-signaling pathways to sense and transduce parasitic signals (14–16). Indeed, the heterotrimeric G-protein  $\alpha$ -subunit  $\alpha$ -gustducin is critical to mounting a type 2 immune response to *T. muris* (8) and to the succinic acid-producing bacteria (12) whereas a transient receptor potential ion channel, Trpm5, is required for tuft cells to turn on the circuit in response to *T. muris* and to the altered microflora (8, 12). It is, however, still unknown how the low number of tuft cells are maintained during the rapid intestinal epithelial cell turnover in the absence of any parasites or their metabolites.

In this study, we identified and functionally characterized Tas2r receptors and other key signaling components utilized by tuft cells in response to one of the parasitic helminths, *Trichinella spiralis* (*Ts*), and provided a more comprehensive understanding of the molecular mechanisms that may underlie the initiation of type 2 immune responses upon infection.

## Significance

Intestinal tuft cells are sentinels monitoring the luminal contents and play a critical role in type 2 immunity. In this work, *Trichinella spiralis* excretion–secretion and extract were shown to directly induce interleukin 25 (IL-25) release from the intestinal villi, evoke calcium responses in tuft cells, and activate Tas2r bitter-taste receptors, whereas the bitter compound salicin was shown to activate and induce tuft cells to release IL-25. G $\alpha$ -gustducin/G $\beta 1\gamma 13$  and/or G $\alpha$ /G $\beta 1\gamma 13$ , Plc $\beta 2$ , I $p_{3r2}$ , and Trpm5 comprise the signal transduction pathways that tuft cells utilize to initiate type 2 immune responses. Potentiation of Trpm5 by a natural sweet compound, stevioside, can enhance the tuft cell–ILC2 circuit's activity, indicating that modulating these signaling components can help devise new means of combating parasites.

Author contributions: X.-C.L. and L.H. designed research; X.-C.L., Z.-H.C., J.-B.X., D.-X.Z., C.L., Y.-H.L., S.-M.L., Y.-W.D., Q.L., P.W., M.L., and L.H. performed research; X.-C.L., Z.-H.C., and L.H. analyzed data; and X.-C.L., Z.-H.C., and L.H. wrote the paper.

The authors declare no conflict of interest.

This article is a PNAS Direct Submission.

This open access article is distributed under Creative Commons Attribution-NonCommercial-NoDerivatives License 4.0 (CC BY-NC-ND).

<sup>1</sup>To whom correspondence should be addressed. Email: huangliqun@zju.edu.cn.

This article contains supporting information online at [www.pnas.org/lookup/suppl/doi:10.1073/pnas.1812901116/-DCSupplemental](http://www.pnas.org/lookup/suppl/doi:10.1073/pnas.1812901116/-DCSupplemental).

Published online February 28, 2019.

## Results

***T. spiralis* Infection Triggers Tuft- and Goblet-Cell Hyperplasia in the Mouse Duodenum, Jejunum, and Ileum.** Since different parasitic helminths have their preferred habitats and thus evoke the host's immune responses in different tissues (17), we set out to determine the extent to which each segment of the mouse small intestine remodels its epithelium following the helminth invasion. Two weeks postoral inoculation of 400 *Ts* muscle larvae into each mouse, each small intestine was fixed, sectioned, and stained with an antibody against a tuft-cell marker, doublecortin-like kinase 1 (*Dclk1*), and with AlnIn blue-nuclear fast red to visualize goblet cells, respectively. Significant increases in the numbers of tuft and goblet cells as well as the size of goblet cells were found in all proximal, middle, and distal segments of the small intestine (*SI Appendix, Figs. S1 and S2*).

***T. spiralis* Activates Bitter-Taste Receptors (*Tas2rs*) on Tuft Cells.** Tuft cells are found to express many taste signal transduction components and have been postulated to act as sentinels to monitor and respond to infectious pathogens (18). We hypothesized that the *Tas2r* bitter-taste receptors may be able to sense the parasitic helminths. To test this hypothesis, we prepared mouse small intestinal villi, stimulated them with the excretion–secretion (E–S) and extracts of *Ts* muscle larvae and adult worms, and then measured the IL-25 released from the villi. The results showed that both the extracts and E–S elicited significantly more IL-25 than the vehicle-treated control (Fig. 1*A* and *SI Appendix, Fig. S3*). However, when the villi were pretreated with a bitter-taste receptor inhibitor, allyl isothiocyanate (AITC), a component of mustard oil (19, 20), *Ts* extract-induced release of IL-25 was significantly reduced (Fig. 1*A*). To further confirm the activation of tuft cells by *Ts* products, we prepared intestinal organoids from a gene knock-in mouse line, *Trpm5-lacZ*, in which the *lacZ*-encoded  $\beta$ -galactosidase is faithfully expressed in the cells normally expressing *Trpm5*. Tuft cells in the organoids from the *Trpm5-lacZ*<sup>+/-</sup> heterozygous mice containing one copy of an intact *Trpm5* gene and one copy of the *lacZ* gene were then identified by their red fluorescence from the compound 2-dodecylresorufin in the cells after incubation with the

ImaGene Red  $\beta$ -galactosidase substrate dodecylresorufin  $\beta$ -D-galactopyranoside (Fig. 1*B* and *C, Insets*). Cells were then loaded with the Ca<sup>2+</sup>-sensitive dye Fluo-4 AM and stimulated with *Ts* extract or E–S products. Transient increases in intracellular Ca<sup>2+</sup> concentrations were observed in the red cells, indicating that *Trpm5*-expressing tuft cells responded to both *Ts* extract and E–S products (Fig. 1*B* and *C* and *SI Appendix, Fig. S4*).

To assess *Tas2r* expression in the small intestine and any changes in its expression during type 2 immune response to *Ts* infection, we carried out reverse transcription–qPCR (RT–PCR) assays with RNAs prepared from the intestines with or without *Ts* infection. The results showed that, among all 35 mouse *Tas2r* genes, the expression of 8 *Tas2rs*—*Tas2r108*, *Tas2r110*, *Tas2r114*, *Tas2r117*, *Tas2r122*, *Tas2r130*, *Tas2r136*, and *Tas2r143*—was significantly up-regulated, 8 others significantly down-regulated, and the remaining 19 unchanged (Fig. 1*D* and *SI Appendix, Figs. S5 and S6*).

Since mouse small intestinal villi contain not only epithelial cells but also immune cells and others (21), small intestinal organoids possess much enriched epithelial cells originating from the *Lgr5*-expressing stem cells in the gut (22). To obtain more accurate expression data from tuft cells, we again performed qPCR assays with the cultured small intestinal organoids following the IL-13 treatment that remarkably increases tuft-cell abundance (*SI Appendix, Fig. S4*). The results showed that IL-13 treatment significantly up-regulated the expression of 3 *Tas2rs*—*Tas2r117*, *Tas2r136*, and *Tas2r143*—11 others significantly down-regulated, and the remaining 21 *Tas2rs* unchanged (Fig. 1*E* and *SI Appendix, Fig. S5*). Meanwhile, expression of the tuft-cell marker genes *Par2*, *Dclk1*, and *Sucnr1* was also significantly up-regulated (*SI Appendix, Fig. S5*), consistent with the tuft-cell hyperplasia (*SI Appendix, Fig. S1*). To confirm the expression of these *Tas2rs* in tuft cells, in situ hybridization was performed on small intestinal sections followed by immunostaining with the *Dclk1* antibody. The results indicated that individual *Tas2r* gene transcripts were localized to subsets of tuft cells (*SI Appendix, Fig. S7*).

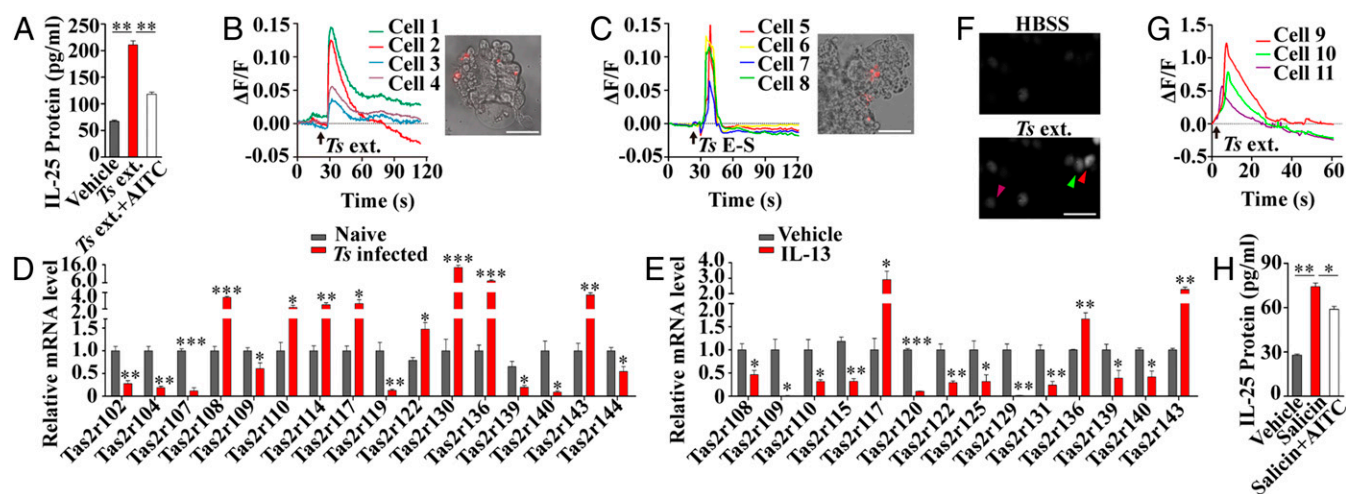


**Fig. 1.** *Tas2r* receptors sense and initiate the response to the helminth *T. spiralis*. (*A*) *Ts* extract of muscle larvae (*Ts* ext.) stimulated the small intestinal villi to release significantly more IL-25 than the vehicle treatment; preincubation with AITC (*Ts* ext.+AITC) significantly reduced IL-25 release ( $n = 4$ ). Representative traces of Ca<sup>2+</sup> responses to *Ts* ext. (*B*) and to *Ts* E–S (*C*) are shown from tuft cells of small intestinal organoids derived from a *Trpm5-lacZ* heterozygous mouse. Red fluorescence was used to identify tuft cells (*Insets*). (*D*) qPCR showed that *Ts* infection increased expression of eight *Tas2rs*—*Tas2r108*, *Tas2r110*, *Tas2r114*, *Tas2r117*, *Tas2r122*, *Tas2r130*, *Tas2r136*, and *Tas2r143*—and down-regulated eight others in the small intestinal villi. (*E*) qPCR showed that IL-13 treatment increased expression of 3 *Tas2rs*—*Tas2r117*, *Tas2r136*, and *Tas2r143*—and down-regulated 11 others in the intestinal organoids. (*F*) Fluorescent images of the Ca<sup>2+</sup>-sensitive dye Fluo-4 AM-loaded HEK293 cells cotransfected with *Tas2r143/Gα16-gust44* with a cotransfection efficiency of 80%, before (HBSS) and after *Ts* ext. stimulation (*Ts* ext.). About 28% of the Fluo-4 AM-loaded cells responded to *Ts* ext. Three representative responding cells are marked by arrowheads. (*G*) Traces of Ca<sup>2+</sup> responses from the three marked cells in *F*. (*H*) Salicin stimulation released significantly more IL-25 than the vehicle treatment from the small intestinal villi; preincubation with AITC (Salicin+AITC) significantly reduced IL-25 release. \* $P < 0.05$ ; \*\* $P < 0.01$ ; \*\*\* $P < 0.001$ . (Scale bars, 50  $\mu$ m.)

In an attempt to predict the up-regulated Tas2rs' ligands, we performed phylogenetic analysis against human TAS2Rs. The results revealed that the eight mouse Tas2rs up-regulated by *Ts* infection show high diversity in amino acid sequences from one another but display certain similarity with some human bitter receptors; in particular, mouse Tas2r143 has a high-level identity to human TAS2R16 (*SI Appendix*, Fig. S8). Further, we carried out receptor protein structure modeling and found that all these 8 Tas2rs have very different predicted receptor structures (*SI Appendix*, Fig. S8). However, the predicted mouse Tas2r143 has a nearly identical receptor structure to that of human TAS2R16. Since Tas2r143 is expressed in tuft cells (23) and human TAS2R16 can be activated by a bitter compound, salicin (24), we reasoned that salicin may be able to activate Tas2r143 on mouse intestinal tuft cells. Indeed, both *Ts* extract and salicin activated heterologously expressed mouse Tas2r143 receptors, which were inhibited by AITC (Fig. 1*F* and *G* and *SI Appendix*, Fig. S9). Furthermore, salicin evoked calcium responses from tuft cells of small intestinal organoids and induced IL-25 release from the intestinal villi, which were Trpm5-dependent and inhibited by AITC (Fig. 1*H* and *SI Appendix*, Fig. S10).

**Tuft Cells Use the Trimeric G Proteins  $\alpha$ -Gustducin/ $G\beta 1\gamma 13$  and  $G\alpha 0$ / $G\beta 1\gamma 13$  to Mediate the Responses to the Parasitic Helminths.** Previous studies have shown that the *Gnat3*-encoded G-protein  $\alpha$ -subunit  $\alpha$ -gustducin is involved in the response to the protist *T. muris* and to the bacteria-produced succinate (8, 12). To determine whether other G-protein subunits also contribute to tuft-cell responses, we performed qPCR to analyze the expression of the genes for all known  $\alpha$ ,  $\beta$ , and  $\gamma$  subunits as well as their variants *Gnao1-A* and *Gnao1-B* in the villi isolated from the mouse duodenums with or without *Ts* infection. Comparative analyses revealed that *Ts* infection resulted in significant increases in expression of three  $G\alpha$  genes—*Gnao1-B*, *Gnat3*, and *Gna15*—but in decreased expression for nine other  $G\alpha$  genes with the remaining four  $G\alpha$  genes unchanged (Fig. 2*A* and *SI Appendix*, Fig. S11). As to G-protein  $\beta\gamma$  subunits, *Ts* infection significantly increased the expression of *Gnb5*, *Gng7*, and *Gng13*, but reduced 4 others with the remaining 9 unaffected (Fig. 2*A* and *SI Appendix*, Fig. S11).

The qPCR analysis with the intestinal organoids showed that IL-13 treatment dramatically increased the expression of *Gnao1-B*, *Gnat3*, *Gna15*, *Gnb5*, and *Gng13* in the duodenal organoids (Fig. 2*B*). In addition, IL-13 treatment also augmented the expression of *Gnb1* by 20.9-fold, which was unchanged in the *Ts*-infected duodenums. Further comparison of the data revealed that *Gnaz* and *Gnat2* were down-regulated in both the *Ts*-infected villi and the IL-13-treated organoids, but an additional four genes were down-regulated only by IL-13 treatment; and conversely, 11 other genes were down-regulated only in the *Ts*-infected villi. *Gnat1* and *Gng1* expression was undetectable in the villi but detectable in the organoids; nevertheless, their expression was unaffected by the IL-13 treatment (Fig. 2 and *SI Appendix*, Fig. S11).

To confirm the qPCR data and to localize the proteins of the genes up-regulated by the *Ts* infection and IL-13 treatment, we carried out immunostaining on mouse small intestinal sections with antibodies against  $\alpha$ -gustducin, Dclk1, and other proteins encoded by the up-regulated genes (Fig. 2 and *SI Appendix*, Fig. S12). As reported previously,  $\alpha$ -gustducin and Dclk1 are colocalized to a subset of small intestinal epithelial cells (Fig. 2*C*) (8). Interestingly, an antibody that can bind to both A and B isoforms of  $G\alpha 0$ , encoded by *Gnao1-A* and *-B*, respectively, costained some tuft cells with the Dclk1 antibody while some epithelial cells were stained by the  $G\alpha 0$  antibody alone, indicating that  $G\alpha 0$  is expressed not only in tuft cells but also in some other Dclk1-negative epithelial cells (Fig. 2*D*). In contrast, the antibody against *Gna15*-encoded  $G\alpha 15$  stained cells in the lamina propria without overlapping with Dclk1 staining at all, indicating that  $G\alpha 15$ -expressing cells were not tuft cells or even epithelial cells (Fig. 2*E*). Double immunostaining also showed that both

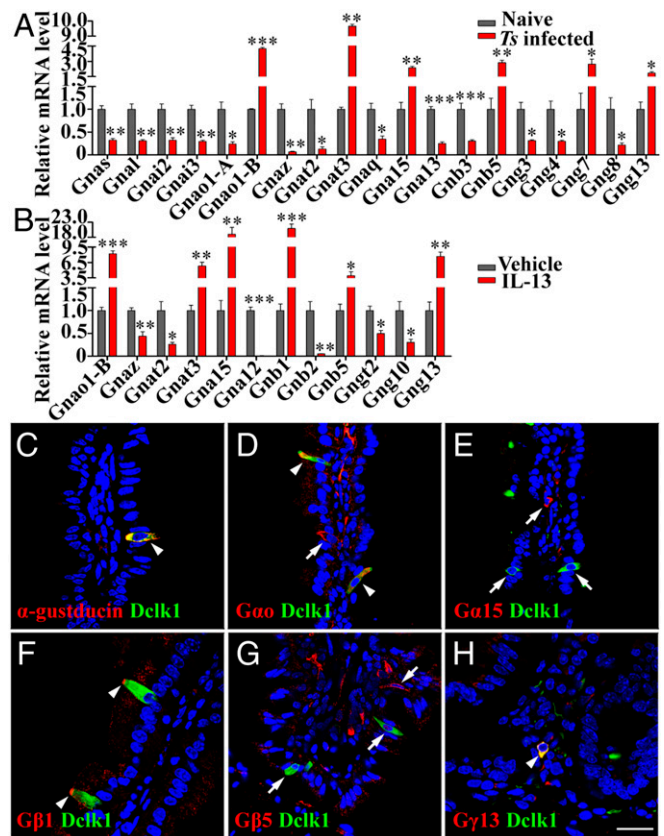


**Fig. 2.** Intestinal tuft cells highly express  $G\alpha 0$ ,  $\alpha$ -gustducin,  $G\beta 1$ , and  $G\gamma 13$ . (A) *Ts* infection altered G-protein subunit expression in the small intestinal villi. qPCR analyses show that *Ts* infection for 2 wk significantly increased the expression of *Gnao1-B*, *Gnat3*, *Gna15*, *Gnb5*, *Gng7*, and *Gng13*, but decreased 13 others. (B) IL-13 treatment of the intestinal organoids up-regulated the expression of *Gnao1-B*, *Gnat3*, *Gna15*, *Gnb1*, *Gnb5*, and *Gng13* but decreased 6 others. \* $P < 0.05$ ; \*\* $P < 0.01$ ; \*\*\* $P < 0.001$ . (C–H) Images of double immunostaining show that Dclk1 (green) is overlapped with  $\alpha$ -gustducin,  $G\alpha 0$ ,  $G\beta 1$ , and  $G\gamma 13$  (arrowheads in C, D, F, and H) but not with  $G\alpha 15$  or  $G\beta 5$  (arrows in E and G). Note: one epithelial cell expressed  $G\alpha 0$  but not Dclk1 (D, arrow) while  $G\beta 1$  was enriched at the tips of tuft cells (F, arrowhead). (Scale bar, 20  $\mu$ m).

$G\beta 1$  and  $G\gamma 13$  but not  $G\beta 5$  are colocalized with Dclk1, indicating that  $G\beta 1\gamma 13$  subunits are expressed in tuft cells (Fig. 2*F–H*). Notably,  $G\beta 1$  proteins seemed to be concentrated at the tip of tuft cells (Fig. 2*F*).

To validate the role of these up-regulated G-protein subunits in tuft-cell physiology, we performed IL-25 ELISAs on the small intestinal villi with the *Ts* extract in combination with G-protein-specific pharmacological agents. Similar to the results shown in Fig. 1*A*, *Ts* extract evoked the small intestinal villi to release IL-25. However, preincubation with pertussis toxin, an inhibitor specifically for the G-protein  $\alpha 0/i$  subfamily, or with a myristoylated peptide inhibitor specifically for  $G\alpha 0$  (25), blocked *Ts* extract-induced release of IL-25 (Fig. 3*A* and *B*). Similarly, the  $G\beta\gamma$ -subunit inhibitor gallein also inhibited the IL-25 release from *Ts* extract-evoked villi (Fig. 3*C*).

To genetically verify  $G\beta 1\gamma 13$ 's role in the regulation of IL-25 release from tuft cells, we took advantage of a conditional gene knockout mouse line, *Lgr5-EGFP-IRES-CreERT2:Gng13<sup>flox/flox</sup>*, which was generated by crossing the *Lgr5-EGFP-IRES-CreERT2* (26) mouse with the *Gng13<sup>flox/flox</sup>* mouse (27). Tamoxifen administration rendered CreERT2 recombinase activity in the *Lgr5*-expressing stem cells in the gut, abolishing  $G\gamma 13$  expression in tuft cells (*SI Appendix*, Fig. S13). ELISAs showed that *Ts* extract-evoked release of IL-25 from the *Gng13<sup>-/-</sup>* villi was significantly

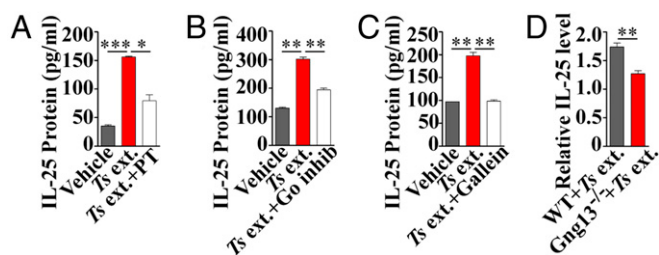


**Fig. 3.** G-protein inhibitors and *Gng13* knockout abolish tuft-cell response to *Ts* extract. *Ts* ext. evoked the release of significantly more IL-25 from the intestinal villi compared with vehicle control. Preincubation with the *Gai/o* inhibitor pertussis toxin (PT) (A), *Gao* peptide inhibitor (Go inhib) (B), or *Gβγ* inhibitor gallein (C) significantly reduced *Ts* ext.-induced IL-25 release. (D) Tamoxifen-induced *Gng13* knockout in the *Lgr5*-EGFP-IRES-CreERT2: *Gng13*<sup>flox/flox</sup> mice significantly reduced *Ts* ext.-induced IL-25 release compared with WT control. \**P* < 0.05; \*\**P* < 0.01; \*\*\**P* < 0.001.

reduced compared with WT control (Fig. 3D), indicating that *Gγ13* is critical to the IL-25 release from tuft cells. To further confirm *Gβ1γ13*'s contribution to type 2 immune response in vivo, another *Gng13*<sup>-/-</sup> mouse line, *Vil1*-Cre:*Gng13*<sup>flox/flox</sup>, was generated by crossing the *Vil1*-Cre mouse (28) with the *Gng13*<sup>flox/flox</sup> mouse, nullifying the *Gng13* expression in the small intestine constitutively. *Ts* infection resulted in much reduced tuft-cell hyperplasia in the knockout small intestines compared with WT control (SI Appendix, Figs. S13 and S14).

**The *Plcβ2*-*Ip3r2* Axis Is Part of the Tuft-Cell Intracellular Signaling Cascade.** The G-protein *β1γ13* dimer is known to activate *Plcβ2* to generate the second messengers inositol 1,4,5-triphosphate (*IP3*) and diacylglycerol whereas *IP3* binds to its receptor on the endoplasmic reticulum (ER), releasing *Ca*<sup>2+</sup> ions from the ER into the cytoplasm and elevating the cytoplasmic free *Ca*<sup>2+</sup> concentration (29). *Plcβ2* is found to be expressed in tuft cells (Fig. 4A). To test *Plcβ2*'s role in tuft cells, we evaluated the effect of the *Plcβ2* inhibitor U73122 on the *Ts* extract-induced IL-25 release. Preincubation with U73122 significantly reduced the amount of IL-25 released from the villi in response to *Ts* extract compared with that without U73122 (Fig. 4B).

To determine which *IP3* receptor subtype is activated by *IP3*, we performed immunostaining with the antibodies against the receptor subtypes *Ip3r2* and *Ip3r3*. Double immunostainings showed that *Ip3r2* was nearly completely overlapped with *Dclk1* in tuft cells (Fig. 4C). In contrast, no overlapping was observed between *Ip3r3* and *Dclk1* on the intestinal epithelial cells, and *Ip3r3* immunostaining was restricted mostly to the lamina propria (Fig. 4D and SI Appendix, Fig. S15). Thus, unlike taste-bud cells that employ *Ip3r3* to transduce taste signals, tuft cells use *Ip3r2* to convey the parasitic signals forward.

**Potentiation of *Trpm5* Facilitates the Activation of the Tuft Cell-ILC2 Circuit.** *Trpm5* is coexpressed with *Dclk1* in tuft cells (8); thus, the *lacZ* gene in the *Trpm5*-*lacZ* knockin mice is colocalized with *Dclk1* in tuft cells (SI Appendix, Fig. S16). To determine whether *Ts*-induced IL-25 release from tuft cells requires *Trpm5*, we quantified the released IL-25 from the small intestinal villi of WT vs. *Trpm5*-knockout/*lacZ*-knockin mice (*Trpm5*<sup>-/-</sup>). Results showed that *Trpm5*<sup>-/-</sup> significantly reduced *Ts* extract-induced IL-25 release compared with WT control (Fig. 4E). Furthermore, *Ts* infection significantly increased tuft-cell abundance in WT but not in *Trpm5*<sup>-/-</sup> mice (SI Appendix, Fig. S17), indicating that *Trpm5* is required for *Ts*-induced IL-25 release and tuft-cell hyperplasia.

To further elucidate *Trpm5*'s role in type 2 immune response, we incubated the small intestinal villi with a *Trpm5* potentiator, stevioside, a noncaloric sweet-tasting compound present in the plant *Stevia rebaudiana* (30). The results showed that stevioside elicited significantly more IL-25 from WT than from *Trpm5*<sup>-/-</sup>

villi, which is similar to the effect of *Ts* extract on these two types of villi (Fig. 4E and F). Furthermore, oral administration of stevioside engendered tuft- and goblet-cell hyperplasia in the small intestine, similar to the effect of 5 mM succinate (12) (Fig. 4G and SI Appendix, Figs. S18–S22).

Previous studies have shown that many cytokines are released from the intracellular stores via vesicular secretion (31). To determine whether IL-25 is also secreted from tuft cells, a vesicular transport inhibitor, brefeldin A (BFA) (32), was used to preincubate the small intestinal villi. The results showed that BFA significantly reduced the IL-25 release from tuft cells in response to *Ts* extract (SI Appendix, Fig. S23).

## Discussion

**Pathogens and Tuft Cells.** Recent studies have shown that tuft cells can detect and respond to multiple types of pathogens, including bacteria, protists, and nematodes. Parasitic helminths may have different preferred habitats inside their hosts, thus stimulating tuft cells residing in particular locations (33). Our data show that *Ts* infection incurred tuft- and goblet-cell expansion throughout the proximal, middle, and distal segments of the small intestine (SI Appendix, Figs. S1 and S2), which is consistent with the expansion caused by the other two helminths studied so far, *N. brasiliensis* and *H. polygyrus*. However, both *Ts* and *N. brasiliensis* can provoke a 10-fold increase in tuft-cell abundance whereas *H. polygyrus* is able to provoke a 5-fold increase (9). The difference in effectiveness can be a result from tripartite interactions among parasitic worms, enteric microflora, and gut cells (12, 33–36). It is also possible that tuft cells express multiple sets of receptors to sense different infectious agents, prompting host cell responses at different intensities. Further studies are needed to understand the underlying molecular mechanisms.

**Tas2r Receptors Are Tuft-Cell Sensors for *T. spiralis*.** Many taste-signaling proteins have been found in tuft cells. However, there was no strong evidence supporting the role of *Tas2rs* in the tuft

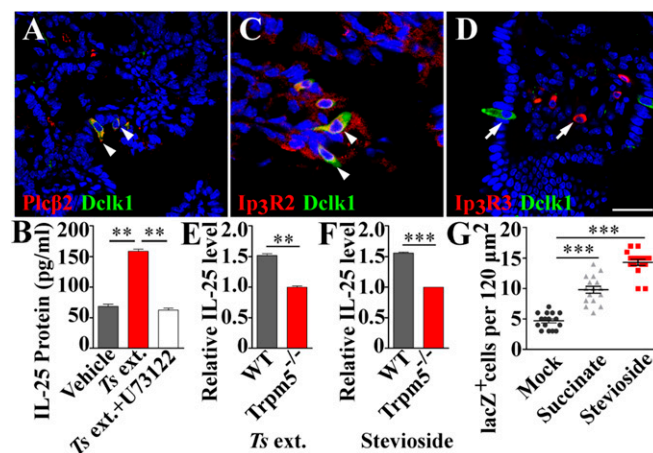


**Fig. 4.** Tuft cells utilize the *Plcβ2*-*Ip3r2*-*Trpm5*-signaling pathway to transduce parasitic signals. (A) Double immunostaining on intestinal sections shows the colocalization of *Plcβ2* (red) with *Dclk1* (green) to tuft cells. (B) *Ts* ext. significantly increased the release of IL-25 from the intestinal villi compared with the vehicle control whereas preincubation with the phospholipase C inhibitor U73122 significantly reduced the IL-25 release. (C and D) Double immunostaining shows that *Ip3r2* (C, red), but not *Ip3r3* (D, red), is coexpressed with *Dclk1* (green) in intestinal tuft cells. Instead, *Ip3r3* is expressed in the lamina propria. (Scale bar, 20 μm.) (E and F) ELISAs show that both *Ts* ext. and 124 μM stevioside stimulated WT but not *Trpm5*<sup>-/-</sup> duodenal villi to release IL-25. (G) Both 5 mM succinate and 0.5 mM stevioside, but not water in the mock treatment, significantly increased tuft-cell abundance in the duodenums of *Trpm5*-*lacZ*<sup>+/-</sup> mice. \*\*\**P* < 0.01; \*\*\*\**P* < 0.001.

cell–ILC2 circuit. In this study, we have shown that both *Ts* muscle larva and adult worm extracts as well as E–S products can elicit not only  $\text{Ca}^{2+}$  responses from tuft cells but also stimulate small intestinal villi to release IL-25, which was blocked by AITC (Fig. 1 A–C and *SI Appendix*, Figs. S3 and S4), strongly suggesting that the Tas2rs are critical to sensing and initiating type 2 immunity. qPCR assays indicated that *Ts* infection and IL-13 treatment up-regulated the expression of 8 and 3 Tas2rs, down-regulated 8 and 11 others, and left 19 and 21 unaltered in the small intestinal villi and organoids, respectively, whereas expression of tuft-cell marker genes was significantly increased, indicating robust tuft-cell hyperplasia in both *Ts*-infected intestine villi and IL-13–treated organoids (Fig. 1 D and E and *SI Appendix*, Figs. S4 and S5). The up-regulated Tas2rs were likely expressed in the expanded tuft cells, while the down-regulated ones were expressed in the lesser represented cells with the unchanged ones possibly expressed in the cells of unchanged representation. However, *Ts* infection augmented the expression of eight *Tas2rs* in the villus cells while IL-13 treatment increased only three of these eight *Tas2rs* in the organoids. This discrepancy may be attributable to the differences in tuft-cell types contained in the two samples: the intestinal villus sample may contain more types of tuft cells while the organoids had fewer types due to their limited number of organoid cells. Our in situ hybridization data and previous reports have shown that individual *Tas2r* genes are expressed in subsets of tuft cells that can be divided into additional types (*SI Appendix*, Fig. S7) (16, 23, 37). In addition, the villus sample also contained other cells, such as immune cells, whereas the organoids consisted of mostly epithelial cells. The same reasons can also explain the discrepancies in the down-regulated *Tas2rs* between the *Ts*-infected intestinal villi and the IL-13–treated organoids.

Homolog analysis found that the eight up-regulated *Tas2rs* possess very diverse sequences (*SI Appendix*, Fig. S8), but some of them share high similarities with some human TAS2Rs. Computational modeling showed that mouse *Tas2r143* is structurally similar to human TAS2R16 (*SI Appendix*, Fig. S8). Interestingly, *Ts* extract can indeed stimulate the heterologously expressed *Tas2r143*, which can also be activated by the human TAS2R16's ligand salicin and inhibited by AITC (Fig. 1 F and G and *SI Appendix*, Fig. S9). Furthermore, salicin can activate tuft cells in the organoids and stimulate IL-25 release from the intestinal villi in an AITC-inhibitable, *Trpm5*-dependent manner (Fig. 1H and *SI Appendix*, Fig. S10). Together, these data indicate that *Tas2r143* plays an important role in *Ts*-evoked tuft-cell release of IL-25. It is possible that the other seven up-regulated *Tas2rs* also respond to *Ts*. However, it remains to be determined whether these receptors also contribute to the initial sensing of *Ts* infection.

*Tas2rs* have been found in many extraoral tissues (38–40), where they detect irritants and bacterial metabolites and regulate immune responses (41, 42). In the gut, these receptors play key roles in the tuft–ILC2 circuit. In addition to *Tas2rs*, however, other receptors, such as those for short-chain fatty acids or succinate, are also essential for intestinal type 2 immunity (12, 43). How these different signaling components orchestrate in tuft cells can be important to the effectiveness of type 2 immunity against pathogens.

**Both  $\text{G}\alpha\text{o}/\text{G}\beta\text{1}\gamma\text{13}$  and  $\text{G}\alpha\text{-gustducin}/\text{G}\beta\text{1}\gamma\text{13}$  Mediate Signal Transduction.** Using the RT-qPCR approach, we discovered that *Ts* infection increased expression of three  $\text{G}\alpha$  genes (*Gnat3*, *Gnao1-B*, and *Gna15*), one  $\text{G}\beta$  gene (*Gnb5*), and two  $\text{G}\gamma$  genes (*Gng7* and *Gng13*) in the small intestine whereas IL-13 treatment also up-regulated gene expression of *Gnat3*, *Gnao1-B*, *Gna15*, *Gnb5*, and *Gng13*. But *Gnb1*, instead of *Gng7*, was up-regulated in the IL-13–treated organoids. The reason that the significant increase of *Gng7* expression in the infected intestine was not observed in the IL-13–treated organoids could be that *Gng7* is expressed in the cells unaffected by IL-13 in the organoids. On the other hand, *Gnb1* is

probably expressed in tuft cells as well as in many other intestinal cells; thus, the increase in its expression contributed by the *Ts*-induced tuft-cell hyperplasia was diluted by its constitutive expression in many other cells and did not reach a statistical significance. In contrast, the intestinal organoids are enriched with epithelial cells including tuft cells, and the increases in the expression of the genes expressed in tuft cells are more readily detected during tuft-cell hyperplasia (*SI Appendix*, Fig. S5).

Immunohistochemical studies showed that  $\text{G}\alpha\text{-gustducin}$ ,  $\text{G}\alpha\text{o}$ ,  $\text{G}\beta\text{1}$ , and  $\text{G}\gamma\text{13}$  are colocalized with *Dclk1* and expressed in tuft cells (Fig. 2). However,  $\text{G}\alpha\text{15}$  and  $\text{G}\beta\text{5}$  are not expressed in tuft cells and thus probably not involved in tuft-cell signal transduction. Notably, similar to sialic-acid-binding Ig-type lectin F (9),  $\text{G}\beta\text{1}$  proteins are enriched at the tip of tuft cells, facilitating coupling of G-protein-coupled receptors (GPCRs) to G proteins. In addition, some  $\text{G}\alpha\text{o}$ -expressing intestinal epithelial cells do not express *Dclk1*, suggesting the existence of *Dclk1*-negative tuft cells (16).

The  $\text{G}\alpha\text{o}/\text{i}$ -,  $\text{G}\alpha\text{o}$ -, and  $\text{G}\beta\gamma$ -specific inhibitors, including pertussis toxin,  $\text{G}\alpha\text{o}$  peptide inhibitor and gallein, respectively, significantly blocked *Ts* extract-induced IL-25 release from the intestinal villi (Fig. 3 A–C), indicating that  $\text{G}\alpha\text{-gustducin}$  and  $\text{G}\alpha\text{o}$ , as well as  $\text{G}\beta\text{1}\gamma\text{13}$  subunits, transduce the parasitic signals and stimulate tuft cells to produce IL-25. Finally, knockout of *Gng13* significantly reduced both *Ts* extract-evoked IL-25 release from the intestinal villi and *Ts* infection-induced tuft-cell hyperplasia, indicating that  $\text{G}\gamma\text{13}$  is a key component of the tuft-cell signaling pathway (Fig. 3D and *SI Appendix*, Fig. S14).

Taken together, our data indicate that both  $\text{G}\alpha\text{o}/\text{G}\beta\text{1}\gamma\text{13}$  and  $\text{G}\alpha\text{-gustducin}/\text{G}\beta\text{1}\gamma\text{13}$  are the heterotrimeric G proteins transducing parasitic signals.  $\text{G}\gamma\text{13}$  has been known to form functional trimeric G proteins with both  $\text{G}\alpha\text{o}$  and  $\text{G}\alpha\text{-gustducin}$ , respectively (44–46). And  $\text{G}\alpha\text{-gustducin}$  has been known to be involved in the succinate- and *T. muris*-evoked type 2 immunity. Given the diversity of pathogens, tuft cells may utilize multiple GPCRs and G proteins to detect and transduce pathogenic signals.

**The  $\text{Plc}\beta\text{2-Ip}_\text{3}\text{r}_\text{2}$  Axis of the Intracellular Signaling Pathway.** *Plc\beta\text{2}* is expressed in tuft cells (8) (Fig. 4A). Pharmacological inhibition of *Plc\beta\text{2}* activity with U73122 significantly reduced *Ts* extract-induced IL-25 release from the intestinal villi (Fig. 4B), indicating that *Plc\beta\text{2}* is an intermediary signaling protein. *Plc\beta\text{2}* in tuft cells is likely to be activated by  $\text{G}\beta\text{1}\gamma\text{13}$ , as in taste-bud cells (45). Activated *Plc\beta\text{2}* generates  $\text{IP}_\text{3}$ , which in turn binds to and opens the channel receptor  $\text{Ip}_\text{3}\text{r}_\text{2}$ , instead of  $\text{Ip}_\text{3}\text{r}_\text{3}$  found in taste-bud cells (Fig. 4 C and D) (29). One difference between  $\text{Ip}_\text{3}\text{r}_\text{2}$  and  $\text{Ip}_\text{3}\text{r}_\text{3}$  is that  $\text{Ip}_\text{3}\text{r}_\text{2}$  has a higher affinity for  $\text{IP}_\text{3}$  but a lower affinity for  $\text{Ca}^{2+}$  (47, 48), suggesting that it can be more readily activated by a smaller amount of  $\text{IP}_\text{3}$  produced by *Plc\beta\text{2}*. From these data, we are inclined to conclude that signaling pathways in tuft cells are more sensitive to sense and to transduce parasitic stimuli than to taste-bud cells to detect sweet, bitter, and umami tastants and that  $\text{Ip}_\text{3}\text{r}_\text{2}$  makes tuft cells more readily or spontaneously active to maintain a basal level of IL-25 and a minimal number of tuft cells in naive mouse intestine and to more rapidly launch a type 2 immune response upon parasite invasion.

***Trpm5* Is a Key Component in the Tuft Cell–ILC2 Circuit.** *Trpm5* is critical to *T. muris* or succinate-elicited type 2 immunity (8, 12). Here we have shown that *Trpm5* is also essential for *Ts*-induced IL-25 release from the intestinal villi as well as for *Ts* infection-evoked tuft-cell hyperplasia (Fig. 4 E–G and *SI Appendix*, Fig. S17). Interestingly, stevioside, a sweet-tasting *Trpm5*'s potentiator, could also elicit IL-25 release from WT but not *Trpm5*<sup>−/−</sup> intestinal cells and trigger tuft-cell hyperplasia in WT but not in *Trpm5*-KO mice (Fig. 4 and *SI Appendix*, Figs. S18 and S19). This effect can be explained by the fact that tuft cells maintain certain levels of basal activity due to  $\text{Ip}_\text{3}\text{r}_\text{2}$ 's intrinsic activity and constant exposure to the plethora of gut microbes, which can be significantly amplified by stevioside. Indeed, 0.5 mM stevioside

seemed to be more potent than 5 mM succinate in launching tuft- and goblet-cell hyperplasia (Fig. 4G and *SI Appendix, Figs. S20 and S21*). Interestingly, stevioside has been used to treat obesity and stomach burn and to increase immune activity (49). But the underlying molecular mechanisms are yet to be elucidated. Our data indicate that Trpm5 is likely the stevioside's target.

Cytokines are known to be released from the cells via several ways, but many of them are through vesicular secretion (31, 32). Our data show that preincubation of the intestinal villi with the vesicular transport inhibitor BFA significantly blocked IL-25 release (*SI Appendix, Fig. S23*), indicating that IL-25 is also secreted via vesicles.

In summary, our results have shown that tuft cells utilize a similar but different signaling pathway from that used by taste-bud cells (*SI Appendix, Fig. S24*): *Ts* molecules activate Tas2rs, which in turn stimulate  $G\alpha$ -gustducin/ $G\beta 1\gamma 13$  or  $G\alpha o$ / $G\beta 1\gamma 13$ ; the G proteins dissociate into  $G\alpha$  and  $G\beta 1\gamma 13$  moieties, and the latter acts on  $Plc\beta 2$ , generating  $IP_3$ ;  $IP_3$  binds to  $IP_3r2$ , releasing  $Ca^{2+}$  from the endoplasmic reticulum into cytosol; the  $Ca^{2+}$  ions open Trpm5, leading to the influx of positively charged  $Na^+$  ions, depolarizing the membrane potential, eventually triggering the vesicular release of IL-25 from tuft cells; IL-25 activates ILC2s,

which produce IL-4 and IL-13; and the cytokines promote the proliferation and differentiation of stem/progenitor cells preferentially into tuft and goblet cells, resulting in tuft- and goblet-cell hyperplasia and consequently weep and sweep responses. Fuller understanding of the molecular mechanisms underlying the tuft cell–ILC2 circuit can provide novel insights into type 2 immunity and help devise new ways to combat widespread parasites.

## Materials and Methods

C57/BL6 mice and Sprague-Dawley rats were purchased from the Shanghai SLAC Laboratory Animal Co. Trpm5-lacZ, Vii1-Cre, and Lgr5-EGFP-ires-CreERT2 mice (Jax stock numbers 005848, 021504, and 008875, respectively) were obtained from the Jackson Laboratory. Studies involving animals were approved by the Zhejiang University Institutional Animal Care and Use Committee. More details about experimental materials and methods are described in *SI Appendix*. The primers used for qPCR are listed in *SI Appendix, Table S1*.

**ACKNOWLEDGMENTS.** We thank Drs. Robert F. Margolskee, Caiyong Chen, and Aifang Du for discussion. This work was supported by grants from the National Natural Science Foundation of China (81671016, 31471008, and 31627801) and the Siyuan Foundation.

- Sansonetti PJ (2004) War and peace at mucosal surfaces. *Nat Rev Immunol* 4:953–964.
- Chow J, Mazmanian SK (2010) A pathobiont of the microbiota balances host colonization and intestinal inflammation. *Cell Host Microbe* 7:265–276.
- Furness JB, Rivera LR, Cho HJ, Bravo DM, Callaghan B (2013) The gut as a sensory organ. *Nat Rev Gastroenterol Hepatol* 10:729–740.
- Öhman L, Törnblom H, Simrén M (2015) Crosstalk at the mucosal border: Importance of the gut microenvironment in IBS. *Nat Rev Gastroenterol Hepatol* 12:36–49.
- Sekirov I, Russell SL, Antunes LC, Finlay BB (2010) Gut microbiota in health and disease. *Physiol Rev* 90:859–904.
- Burrows MP, Volchkov P, Kobayashi KS, Chervonsky AV (2015) Microbiota regulates type 1 diabetes through Toll-like receptors. *Proc Natl Acad Sci USA* 112:9973–9977.
- Wilen CB, et al. (2018) Tropism for tuft cells determines immune promotion of norovirus pathogenesis. *Science* 360:204–208.
- Howitt MR, et al. (2016) Tuft cells, taste-chemosensory cells, orchestrate parasite type 2 immunity in the gut. *Science* 351:1329–1333.
- Gerbe F, et al. (2016) Intestinal epithelial tuft cells initiate type 2 mucosal immunity to helminth parasites. *Nature* 529:226–230.
- von Moltke J, Ji M, Liang HE, Locksley RM (2016) Tuft-cell-derived IL-25 regulates an intestinal ILC2-epithelial response circuit. *Nature* 529:221–225.
- Nadjombati MS, et al. (2018) Detection of succinate by intestinal tuft cells triggers a type 2 innate immune circuit. *Immunity* 49:33–41.e7.
- Lei W, et al. (2018) Activation of intestinal tuft cell-expressed *Sucnr1* triggers type 2 immunity in the mouse small intestine. *Proc Natl Acad Sci USA* 115:5552–5557.
- Schneider C, et al. (2018) A metabolite-triggered tuft cell-ILC2 circuit drives small intestinal remodeling. *Cell* 174:271–284.e14.
- Bezençon C, et al. (2008) Murine intestinal cells expressing Trpm5 are mostly brush cells and express markers of neuronal and inflammatory cells. *J Comp Neurol* 509:514–525.
- Bezençon C, le Coutre J, Damak S (2007) Taste-signaling proteins are coexpressed in solitary intestinal epithelial cells. *Chem Senses* 32:41–49.
- Haber AL, et al. (2017) A single-cell survey of the small intestinal epithelium. *Nature* 551:333–339.
- Mitreva M, Jasmer DP (2006) Biology and genome of *Trichinella spiralis*. *WormBook: The Online Review of C. elegans Biology* (The C. elegans Research Community, Pasadena, CA), pp 1–21.
- Gerbe F, Legrauerend C, Jay P (2012) The intestinal epithelium tuft cells: Specification and function. *Cell Mol Life Sci* 69:2907–2917.
- Oka Y, Butnaru M, von Buchholtz L, Ryba NJ, Zuker CS (2013) High salt recruits aversive taste pathways. *Nature* 494:472–475.
- Barretto RP, et al. (2015) The neural representation of taste quality at the periphery. *Nature* 517:373–376.
- Ramanan D, Cadwell K (2016) Intrinsic defense mechanisms of the intestinal epithelium. *Cell Host Microbe* 19:434–441.
- Sato T, et al. (2009) Single Lgr5 stem cells build crypt-villus structures in vitro without a mesenchymal niche. *Nature* 459:262–265.
- Liu S, et al. (2017) Members of bitter taste receptor cluster *Tas2r143/Tas2r135/Tas2r126* are expressed in the epithelium of murine airways and other non-gustatory tissues. *Front Physiol* 8:849.
- Bufe B, Hofmann T, Krautwurst D, Raguse JD, Meyerhof W (2002) The human TAS2R16 receptor mediates bitter taste in response to beta-glucopyranosides. *Nat Genet* 32:397–401.
- McPherson KB, et al. (2018) Regulators of G-protein signaling (RGS) proteins promote receptor coupling to G-protein-coupled inwardly rectifying potassium (GIRK) channels. *J Neurosci* 38:8737–8744.
- Barker N, et al. (2007) Identification of stem cells in small intestine and colon by marker gene Lgr5. *Nature* 449:1003–1007.
- Li F, et al. (2013) Heterotrimeric G protein subunit Gy13 is critical to olfaction. *J Neurosci* 33:7975–7984.
- Madison BB, et al. (2002) Cis elements of the villin gene control expression in restricted domains of the vertical (crypt) and horizontal (duodenum, cecum) axes of the intestine. *J Biol Chem* 277:33275–33283.
- Hisatsune C, et al. (2007) Abnormal taste perception in mice lacking the type 3 inositol 1,4,5-trisphosphate receptor. *J Biol Chem* 282:37225–37231.
- Philippaert K, et al. (2017) Steviol glycosides enhance pancreatic beta-cell function and taste sensation by potentiation of TRPM5 channel activity. *Nat Commun* 8:14733.
- Stow JL, Murray RZ (2013) Intracellular trafficking and secretion of inflammatory cytokines. *Cytokine Growth Factor Rev* 24:227–239.
- Zhu FG, Gomi K, Marshall JS (1998) Short-term and long-term cytokine release by mouse bone marrow mast cells and the differentiated KU-812 cell line are inhibited by brefeldin A. *J Immunol* 161:2541–2551.
- Bouchery T, et al. (2017) The study of host immune responses elicited by the model murine hookworms *Nippostrongylus brasiliensis* and *Heligmosomoides polygyrus*. *Curr Protoc Mouse Biol* 7:236–286.
- Sartor RB (1997) Review article: Role of the enteric microflora in the pathogenesis of intestinal inflammation and arthritis. *Aliment Pharmacol Ther* 11(Suppl 3):17–22.
- Jiang HY, et al. (2016) Intestinal microbes influence the survival, reproduction and protein profile of *Trichinella spiralis* in vitro. *Int J Parasitol* 46:51–58.
- Fricke WF, et al. (2015) Type 2 immunity-dependent reduction of segmented filamentous bacteria in mice infected with the helminth parasite *Nippostrongylus brasiliensis*. *Microbiome* 3:40, and erratum (2015) 3:77.
- Kok BP, et al. (2018) Intestinal bitter taste receptor activation alters hormone secretion and imparts metabolic benefits. *Mol Metab* 16:76–87.
- Voigt A, et al. (2012) Genetic labeling of Tas1r1 and Tas2r131 taste receptor cells in mice. *Chem Senses* 37:897–911.
- Gu F, et al. (2015) Bitter taste receptor mTas2r105 is expressed in small intestinal villus and crypts. *Biochem Biophys Res Commun* 463:934–941.
- Saunders CJ, Christensen M, Finger TE, Tizzano M (2014) Cholinergic neurotransmission links solitary chemosensory cells to nasal inflammation. *Proc Natl Acad Sci USA* 111:6075–6080.
- Verbeurg C, et al. (2017) The human bitter taste receptor T2R38 is broadly tuned for bacterial compounds. *PLoS One* 12:e0181302.
- Krasteva G, Canning BJ, Papadakis T, Kummer W (2012) Cholinergic brush cells in the trachea mediate respiratory responses to quorum sensing molecules. *Life Sci* 91:992–996.
- Kim MH, Kang SG, Park JH, Yanagisawa M, Kim CH (2013) Short-chain fatty acids activate GPR41 and GPR43 on intestinal epithelial cells to promote inflammatory responses in mice. *Gastroenterology* 145:396–406.e1-10.
- Huang L, et al. (2003) G protein subunit G gamma 13 is coexpressed with G alpha o, G beta 3, and G beta 4 in retinal ON bipolar cells. *J Comp Neurol* 455:1–10.
- Huang L, et al. (1999) Ggamma13 colocalizes with gustducin in taste receptor cells and mediates  $IP_3$  responses to bitter denatonium. *Nat Neurosci* 2:1055–1062.
- Ramakrishnan H, et al. (2015) Differential function of Gy13 in rod bipolar and ON cone bipolar cells. *J Physiol* 593:1531–1550.
- Bezprozvany I (2005) The inositol 1,4,5-trisphosphate receptors. *Cell Calcium* 38:261–272.
- Tu H, Wang Z, Bezprozvany I (2005) Modulation of mammalian inositol 1,4,5-trisphosphate receptor isoforms by calcium: A role of calcium sensor region. *Biophys J* 88:1056–1069.
- Sehar I, Kaul A, Bani S, Pal HC, Saxena AK (2008) Immune up regulatory response of a non-caloric natural sweetener, stevioside. *Chem Biol Interact* 173:115–121.